Engineering with Computers (2022) 38 (Suppl 5):S3901–S3914
https://doi.org/10.1007/s00366-020-01272-9

ORIGINAL ARTICLE

A generalized artificial intelligence model for estimating the friction angle of clays in evaluating slope stability using a deep neural network and Harris Hawks optimization algorithm

Hong Zhang[1] · Hoang Nguyen[2] · Xuan-Nam Bui[2,3] · Biswajeet Pradhan[4,5] · Panagiotis G. Asteris[6] · Romulus Costache[7,8] · Jagannath Aryal[9]

Received: 25 May 2020 / Accepted: 26 December 2020 / Published online: 28 January 2021

Abstract

In landslide susceptibility mapping or evaluating slope stability, the shear strength parameters of rocks and soils and their effectiveness are undeniable. However, they have not been studied for all-natural materials, as well as different locations. Therefore, this paper proposes a novel generalized artificial intelligence model for estimating the friction angle of clays from different areas/locations for evaluating slope stability or landslide susceptibility mapping, including the datasets from the UK, New Zealand, Indonesia, Venezuela, USA, Japan, and Italy. The robustness and consistency of the model's prediction were checked by testing with various datasets having different geological and geomorphological setups. Accordingly, 162 observations from different areas/locations were collected from the locations and regions above for this aim. Subsequently, deep learning techniques were applied to develop the multiple layer perceptron (MLP) neural network model (i.e., DMLP model) with the goal of error reduction of the MLP model. Next, Harris Hawks optimization (HHO) algorithm was applied to boost the optimization of the DMLP model for predicting friction angle of clays aiming to get a better accuracy than those of the DMLP model, called HHO–DMLP model. A DMLP neural network without optimization of the HHO algorithm and two other conventional models (i.e., SVM and RF) were also employed to compare with the proposed HHO–DMLP model. The results showed that the proposed HHO–DMLP model predicted the friction angle of clays better than those of the other models. It can reflect the friction angle of clays with acceptable accuracy from different locations and regions (i.e., MSE = 12.042; RMSE = 3.470; R^2 = 0.796; MAPE = 0.182; and VAF = 78.806). The DMLP model without optimization of the HHO algorithm provided slightly lower accuracy (i.e., MSE = 15.151; RMSE = 3.892; R^2 = 0.738; MAPE = 0.202; and VAF = 73.431). Besides, two other conventional models (i.e., SVM and RF) provided low reliability, especially over-fitting happened with the RF model, and it was not recommended to be used to predict the friction angle of clays (i.e., RMSE = 6.325 and R^2 = 0.377 on the training dataset, but RMSE = 1.669 and R^2 = 0.961 on the testing dataset).

Keywords Clay · Friction angle · Shear strength · Deep learning · Harris hawks optimization

1 Introduction

Landslide and slope stability are major geohazards that need to be handled, predicted, and mapped in worldwide [1–3]. It has an essential significance in controlling the natural hazards induced by landslides and slope instability. Many scholars have succeeded in predicting and mapping landslides based on data science [4–7]. However, soils/rocks shear strength parameters and their effectiveness have not been studied for all-natural materials, as well as different locations [8–10]. Meanwhile, shear strength parameters (e.g., friction angle and cohesion) of natural materials are considered as essential factors in assessing the deformation and stability of geotechnical structures such as slopes, landslide, foundations, dams, and retaining walls [11–14]. Of those, cohesion is taken into account as the most important factor in evaluating the stability of slopes in cases of cemented rocks and soils, and the

Supplementary Information The online version contains supplementary material available at https://doi.org/10.1007/s00366-020-01272-9.

✉ Hoang Nguyen
nguyenhoang@humg.edu.vn

Extended author information available on the last page of the article

friction angle for the cases of uncemented rocks and soils [15–17]. To determine the values of cohesion and friction angle, experiments are usually carried out in laboratories based on standard methods, such as Mohr–Coulomb theory, Bishop [18–20]. Nevertheless, they were recommended in a limited range [21–23]. Furthermore, laboratory experiments are often complex and costly due to the preparation of samples and experimental conditions [24]. In addition, the experimental results often do not reflect all the characteristics of rocks and soils in reality [25, 26]. Therefore, a new method capable of predicting shear strength parameters of rocks and soils in practice with high reliability is a challenge for engineers and scientists.

Regarding the prediction of rocks/soils shear strength parameters, significant efforts have been made in the literature [27, 28]. Garven and Vanapalli [29] evaluated the performance of nineteen empirical methods to forecast the shear strength of unsaturated soils (SSoUS). The suitability of the nineteen empirical equations has been recommended and highlighted for predicting SSoUS. However, these empirical equations resulted into sub-optimal accuracy [30, 31].

To overcome the drawbacks of empirical equations and experimental tests in laboratories, in recent years, artificial intelligence (AI) has been introduced as a robust technique. Many AIs techniques have been successfully applied in practical engineering [32–41]. For predicting friction angle, Das and Basudhar [42] developed an artificial neural network (ANN), and clay was the objective considered in their study. They concluded that ANN could explain the physical effect of clay characteristics and friction angle. In another study, Das et al. [43] developed different AI techniques (e.g., ANN-based and SVM-based) for predicting the friction angle of clay. Finally, the SVM model was confirmed as the best AI technique in their study to predict friction angle of clay. Khan et al. [44] also predicted the friction angle of clay based on the same dataset of Das et al. [43], using a functional network (FN). Their results were then compared with the obtained results in the paper by Das et al. [43] to prove the accuracy of the FN model. Their comparisons indicated that FN model was a good candidate for predicting friction angle of clay. Based on the stochastic approach of the Monte Carlo algorithm, Casagrande et al. [45] successfully predicted the shear strength of rock discontinuities. Positive outcomes were then presented in their study with high reliability. In another study, Pham et al. [46] successfully developed four AI models for predicting shear strength of soft soil, including ANN, SVM, and ANFIS based on particle swarm optimization (PANFIS) and genetic algorithms (GANFIS). Finally, the PANFIS was introduced as the best model for their purposes. Matos et al. [47] also predicted the shear strength of unfilled rock joints based on a novel AI approach, namely the first-order Takagi–Sugeno fuzzy (FOTSF). Eventually, they introduced the FOTSF model as a useful tool to predict the shear strength of unfilled rock joints.

Systematic literature review showed that state-of-the-art AI techniques have been efficiency used and successfully applied terms of shear strength parameters prediction of rocks and soils and their effectiveness are undeniable. However, they have not been studied for all-natural materials, as well as different locations. Moreover, novel AI models with the improved accuracy are always the goal of scientists/researchers. Hence, this work developed and proposed a novel paradigm based on the deep learning technique and optimization algorithm for predicting friction angle of clay. Accordingly, the deep learning techniques were combined with the Harris Hawks optimization (HHO) algorithm to train and develop a multiple layer perceptron (MLP) neural network for this aim, called HHO–DMLP model. An MLP neural network (without optimization), SVM, and random forest (RF) models were then investigated and evaluated with that of the proposed HHO–DMLP model aiming to highlight the obtained results of the HHO–DMLP model.

2 Methodology

The focus of the present study is to propose a novel paradigm based on the hybridization techniques, i.e., HHO–DMLP for predicting friction angle of clay. Therefore, this section only focusses on the details of MLP neural network and HHO algorithm, as well as proposing the framework of the HHO–DMLP model. The detail of SVM and RF can be referred to the following papers [48–53].

2.1 Deep neural network (deep learning for MLP neural network)

As one of the most common types of ANN used in many applications in real life, MLP is well known as a flexible neural network with the structure consists of multiple layers [54, 55]. In each layer, neurons are the main components, and they connect to form a network capable of transmitting the information [56]. The process of transferring information between layers and neurons is performed by training algorithms, such as feed-forward, back-propagation, and Levenberg–Marquardt [57–59]. In MLP neural networks, weights are the main information, and they are used to assess the quality of the network. They have a significant effect on the training performance and accuracy of the network. An MLP neural network with multiple hidden layers is capable of improvement of information between neurons, called deep neural network (DNN) [60].

The concept of DNN has been introduced in recent years for complex issues that require a high degree of accuracy. However, training a DNN to achieve the desired effect is not

easy. Therefore, the concept of deep learning has been introduced and proposed to train DNN to achieve better results [61]. In MLP neural networks, deep learning can perform many tasks to get the optimal network structure, higher accuracy level, faster computing speed, and more stable predictive results [62, 63].

Literature review shows that DNN has been successfully applied in many fields, especially in mining and geotechnical engineering [64–69]. In this study, deep learning was considered training a deep MLP neural network for predicting friction angle of clay, for determining the optimal structure and loss function of the MLP neural network. Besides, the activation functions between layers also play an important role in understanding the connection as well as the performance of the network [70, 71]. Review of the literature shows that the rectified linear activation function (ReLU) has been used as a result in many works [72–76]. By the use of the ReLU activation function, MLP can overcome the problem of vanishing gradient. Furthermore, it allows the MLP model to train faster and get better performance. Thus, it is considered as the most widely used activation function in deep learning models and it works great in most applications. Herein, we used the ReLU active function to discover the connections of neurons in the hidden layers. Also, a linear activation function was applied for the output layer of the network to evaluate the quality of the outcomes. The structure and flowchart of an MLP neural network as well as the activation functions used for predicting friction angle of clay are shown in Fig. 1.

2.2 Harris Hawks optimization (HHO) algorithm

HHO is one of the swarm-based algorithms which was developed by Heidari et al. [77]. Inspired by the predatory behavior of hawks, the HHO algorithm implements strategies to optimize its goals, including two main steps: exploration and exploitation (Fig. 2). In exploration step, Harris Hawks can perch at random locations of other hawks to explore prey. Then, they can apply the soft or hard besieges strategies for attacking the prey (exploitation step) (Fig. 3). In fact, the prey can detect hawk attacks and escape before they are attacked. Therefore, HHO algorithm applied the soft or hard besieges with progressive rapid dives strategies to eliminate the ability of the prey to escape. Figure 2 presents step by step of the HHO algorithm for optimization problems. Please note Eqs. (1–6) in the optimization sequence of the HHO algorithm [77] are presented in supplementary materials. More details of HHO algorithm are described in Heidari et al. (2019).

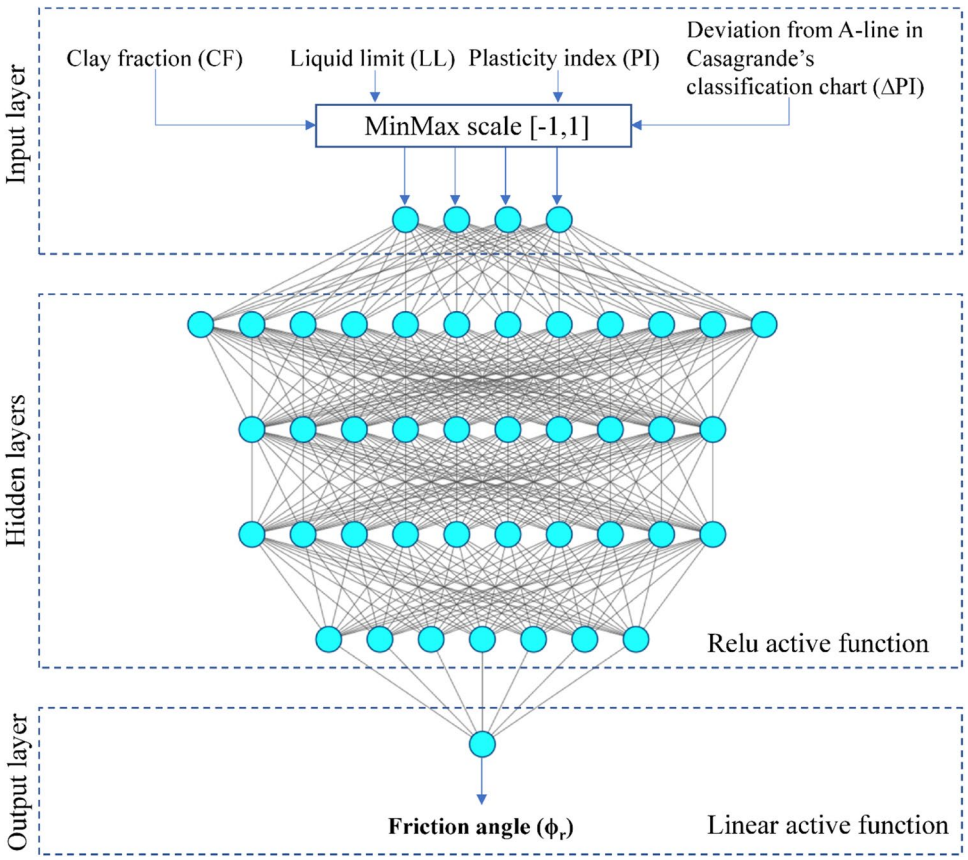

Fig. 1 Structure and flowchart of the MLP neural network for predicting friction angle

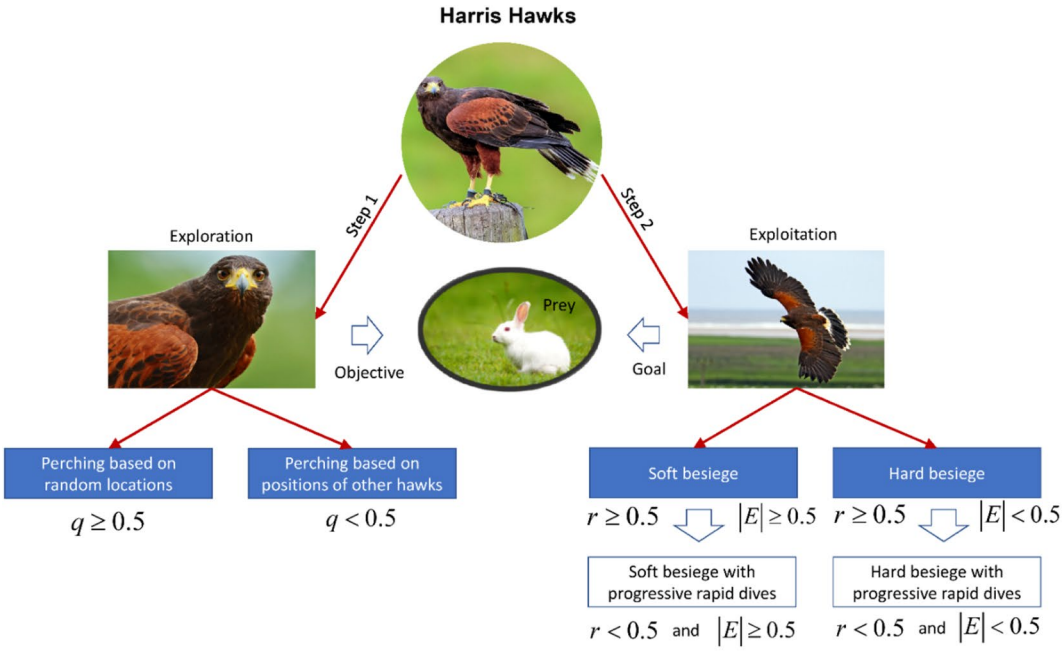

(a)

Algorithm 1 Pseudo-code of HHO algorithm

Inputs: The population size N and maximum number of iterations T
Outputs: The location of rabbit and its fitness value
Initialize the random population $X_i(i = 1, 2, \ldots, N)$
while (stopping condition is not met) **do**
  Calculate the fitness values of hawks
  Set X_{rabbit} as the location of rabbit (best location)
  for (each hawk (X_i)) **do**
    Update the initial energy E_0 and jump strength J ▷ E_0=2rand()-1, J=2(1-rand())
    Update the E using Eq. (1)
    if ($|E| \geq 1$) **then** ▷ Exploration phase
      Update the location vector using Eq. (2)
    if ($|E| < 1$) **then** ▷ Exploitation phase
      if ($r \geq 0.5$ and $|E| \geq 0.5$) **then** ▷ Soft besiege
        Update the location vector using Eq. (3)
      else if ($r \geq 0.5$ and $|E| < 0.5$) **then** ▷ Hard besiege
        Update the location vector using Eq. (4)
      else if ($r < 0.5$ and $|E| \geq 0.5$) **then** ▷ Soft besiege with progressive rapid dives
        Update the location vector using Eq. (5)
      else if ($r < 0.5$ and $|E| < 0.5$) **then** ▷ Hard besiege with progressive rapid dives
        Update the location vector using Eq. (6)
Return X_{rabbit}

(b)

Fig. 2 Mechanism, phases, and the optimization sequence of the HHO algorithm (modified after Heidari et al. [77]). **a** Strategies of Harris Hawks and **b** the optimization sequence of the HHO algorithm

Literature review shows that the HHO algorithm has been successfully applied for many problems [78–82]. Herein, the HHO algorithm was used as a nature-based optimization algorithm for the optimization

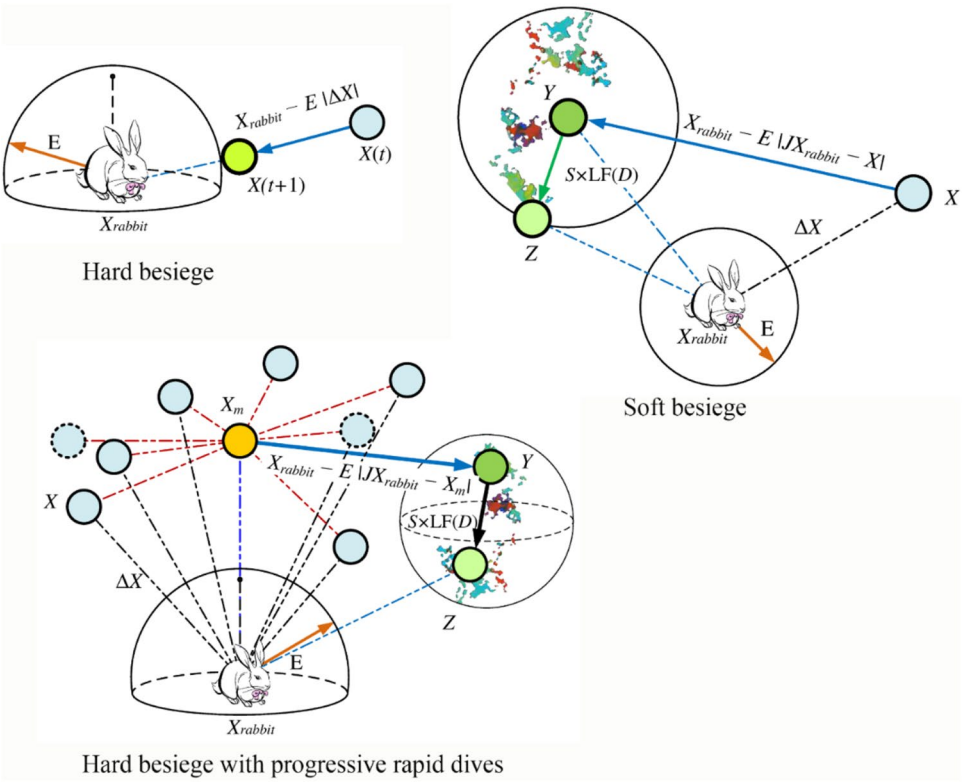

Fig. 3 The strategies of the HHO algorithm [77]

and improvement of a deep MLP neural network (i.e., HHO–DMLP), for predicting friction angle of clay.

2.3 Proposing the framework of HHO–DMLP

To propose the framework of the HHO–DMLP model, three models are prepared: deep learning techniques, MLP neural network, and HHO algorithm. Accordingly, MLP neural network was selected as the key model for predicting friction angle of clay in this study. Deep learning was then applied to finding the optimal structure of the MLP neural network (e.g., hidden layers and neurons). Furthermore, learning rate and batch size of the MLP neural network were also optimized by deep learning. Finally, the HHO algorithm was applied as a meta-learning model to optimize the weight values of the MLP neural network. Herein, MSE was selected as the objective function for deep learning and optimization of the HHO algorithm. The lowest MSE was considered as the best performance of the HHO–DMLP model. The proposed framework of the HHO–DMLP model for forecasting friction angle of clay is introduced in Fig. 4.

3 Data acquisition and preparation

The focus of the present study is to propose a novel paradigm based on the hybridization techniques that can predict and represent for the friction angle of clays at different areas/locations. Therefore, a database containing 162 observations was collected from the previous studies [30, 83–86] at different areas. Four input variables were taken into account to predict friction angle (ϕ_r), including clay fraction (CF), liquid limit (LL), plasticity index (PI), and deviation from A-line in Casagrande's classification chart (ΔPI). The range as well as properties of the collected dataset is listed in Table 1.

Before developing the predictive models, some data analyses are necessary to ensure the accuracy as well as the stability of the models. Based on the properties of the dataset in Table 1, it is clear that the range of all inputs and output is widely varied. They predict a result with great variability in this study. Therefore, scaling features are necessary to make for them to a particular range (e.g., [0,1], [-1, 1]). Also, the correlation between inputs and output should be carefully checked to evaluate the effects of inputs on the output, as well as the overlap of the inputs in the dataset used. A correlation matrix is analyzed in Table 2 to show those points.

In data mining, correlation between variables is a crucial parameter to evaluate the quality of the dataset used, as well as having a good plan for models' development. Accordingly, the acceptable correlation of the variables should be in the range of − 0.8 to 0.8 [32]. It can be seen that most of the variables have an acceptable correlation as shown in Table 2. In particular, the correlation between LL and PI is highest (i.e., 0.782). However, this is still acceptable since their correlation with the other variables

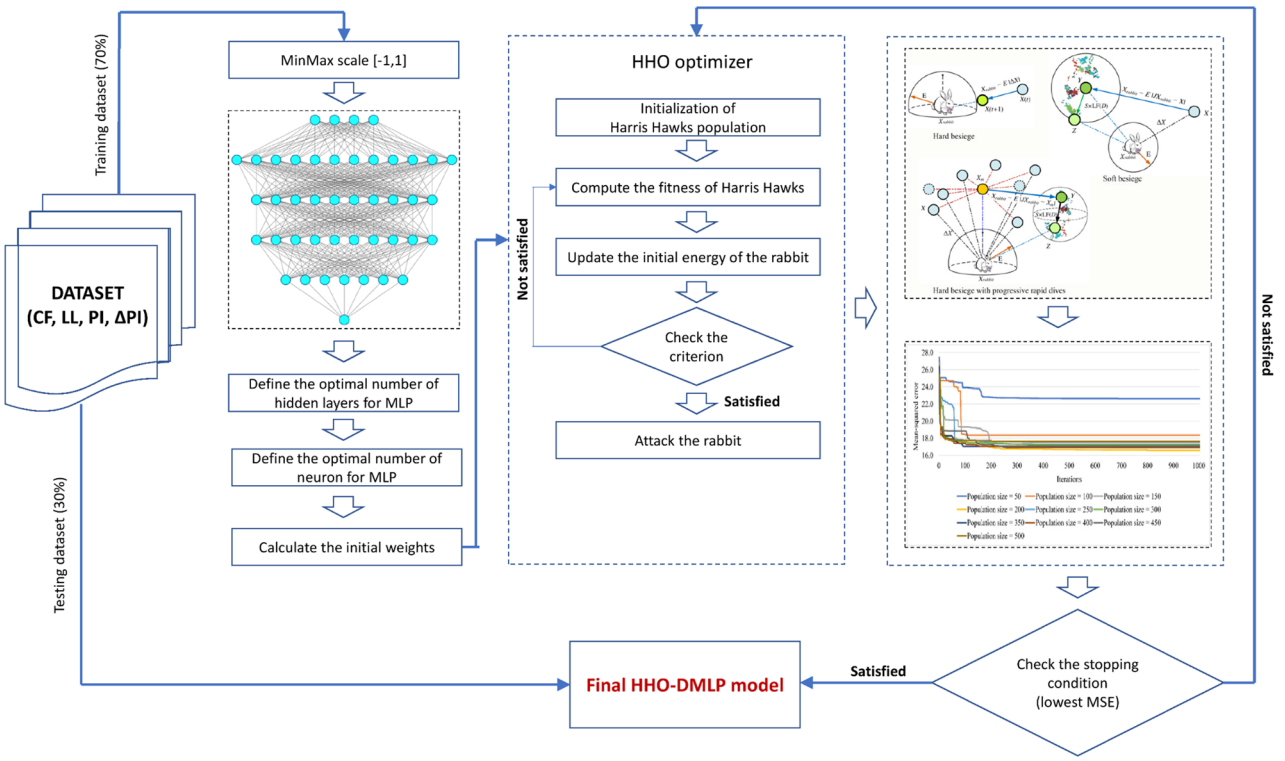

Fig. 4 Introduction of the HHO–DMLP flowchart for forecasting the friction angle of clay in this study

Table 1 Statistical indices of the dataset used

Category	LL	PI	ΔPI	CF	ϕ_r
Min	22	4.5	− 94.89	0.4	4
1st Qu	54	21.68	− 4.197	20	9.825
Median	64	34.05	1.97	32.1	13.05
Mean	67.57	35.08	0.353	33.87	15.502
3rd Qu	78.8	46	7.202	50	19.825
Max	213	132	29.07	91	39

Table 2 Correlation matrix of the friction angle database used

	LL	PI	ΔPI	CF	ϕ_r
LL	1	0.782	− 0.362	0.564	− 0.220
PI	0.782	1	0.297	0.692	− 0.572
ΔPI	− 0.362	0.297	1	0.171	− 0.519
CF	0.564	0.692	0.171	1	− 0.536
ϕ_r	− 0.220	− 0.572	− 0.519	− 0.536	1

Table 3 Statistical indices of the training dataset used

Category	LL	PI	ΔPI	CF	ϕ_r
Min	22	5	− 94.89	0.4	4
1st Qu	54	21.9	− 4.36	20	9.8
Median	66	34.6	1.96	33	12.7
Mean	69.32	36.08	0.07628	35.29	15.34
3rd Qu	80	46	7.44	52	20
Max	213	132	29.07	91	39

Table 4 Statistical indices of the testing dataset used

Category	LL	PI	ΔPI	CF	ϕ_r
Min	26	4.5	− 44.29	1.8	6.4
1st Qu	48.6	20	− 3.37	19.2	10
Median	63	33	1.98	30.2	14.4
Mean	63.54	32.78	0.9912	30.58	15.88
3rd Qu	76	43.9	6.47	45	19
Max	120	83	12.5	76	35

is low, and the value of 0.782 is not too high to remove one of them from the dataset collected. Therefore, we used all four input variables (i.e., LL, PI, ΔPI, and CF) for predicting the friction angle (ϕ_r) in this study.

For training the prediction models, as well as evaluating the performance of the friction angle predictive models in practical engineering, a data split procedure was conducted with 70% of the whole dataset which was used for training

the prediction models, and the remaining 30% was used for evaluation purposes. The details of the datasets are listed in Tables 3 and 4.

4 Results

Once the dataset was well prepared, the procedures for developing friction angle predictive models were applied. In this study, two data scaling methods, such as MinMax and BoxCox, were used to normalize the dataset aiming to avoid over-fitting. Accordingly, the MinMax scaling method was applied during developing the DMLP and HHO–DMLP models, whereas the BoxCox scaling method was applied for the SVM and RF models. To do end, Fig. 4 is applied for developing the HHO–DMLP model. Note that some deep learning techniques were applied to develop the initial MLP neural network model. Accordingly, a deep learning procedure was employed for the selection of the optimal number of hidden layers in the MLP neural network based on the MSE values. To find out the optimal results, 500 epochs were used for this task. Finally, as shown in Fig. 5, the results showed that 3 hidden layers are the best structure for the MLP model in this work.

Once the optimal number of hidden layers is well determined, the optimal number of neurons is also determined based on the similar deep learning techniques in the range of 8–30. Eventually, the optimal number of hidden neurons for each hidden layer was determined as 18, 16, and 8, for the first, second, and third hidden layers, respectively (Fig. 6a). The optimal structure of the MLP neural network was defined as DMLP 4-18-16-8-1, and its performance is illustrated in Fig. 6b.

Once the DMLP model was well defined, the HHO was applied as a robust optimization algorithm to improve the performance of the DMLP model through the weight's

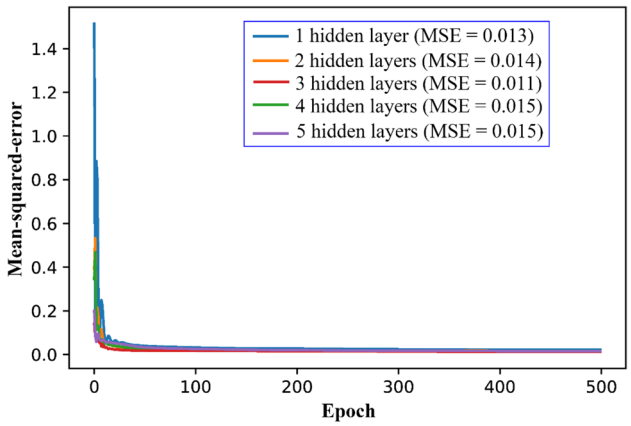

Fig. 5 The error of the MLP paradigm with a different number of hidden layers and epochs

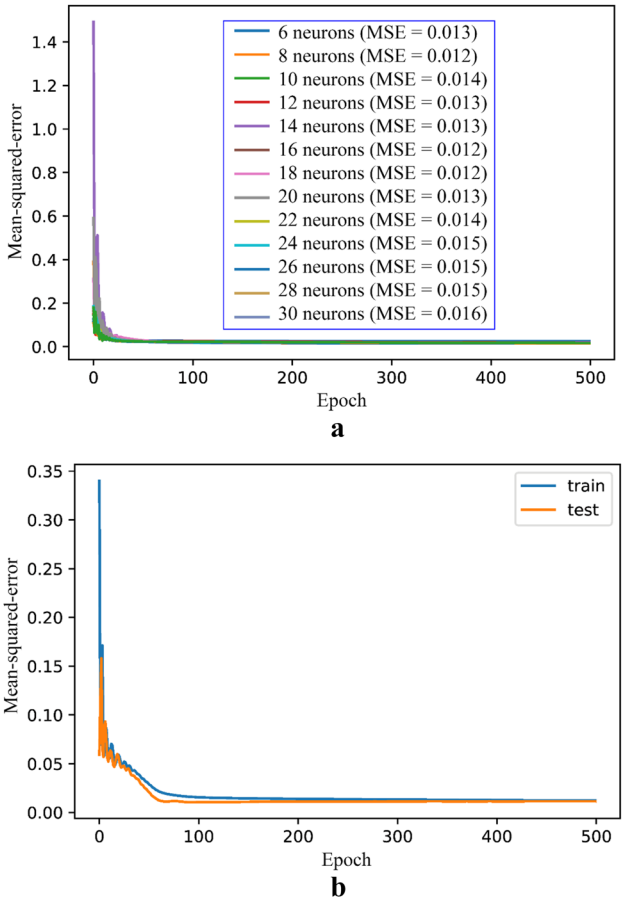

Fig. 6 **a** The error of the MLP neural network with different neurons. **b** The error and performance of the selected deep MLP neural network (DMLP)

adjustment. The different number of Harris Hawks was set as 50, 100, 150, 200, 250, 300, 350, 400, 450, 500 to examine the performance of the HHO algorithm in optimization of the DMLP model. Furthermore, 1000 iterations were established to find out the best result with the lowest MSE for the DMLP model. Figure 7 shows the performance of the HHO algorithm with a different number of Harris Hawks (population size). The results in Fig. 7 show that the DMLP model achieved the optimal value with the population size of 200 at the iteration of 799 (MSE = 13.493).

To prove the performance of the HHO–DMLP model, the DMLP without optimization by the HHO algorithm was also employed based on the same structure and datasets. Furthermore, two forms of the conventional models, namely SVM and RF, were also considered and evaluated in terms of modeling and accuracy to have a comprehensive assessment of the DMLP and HHO–DMLP models. It is worth noting that all the predictive models are developed based on the same training dataset. Herein, radius basis function (RBF) and a grid search of the parameters were applied for the SVM model, whereas 2000 trees and 4 randomly predictors

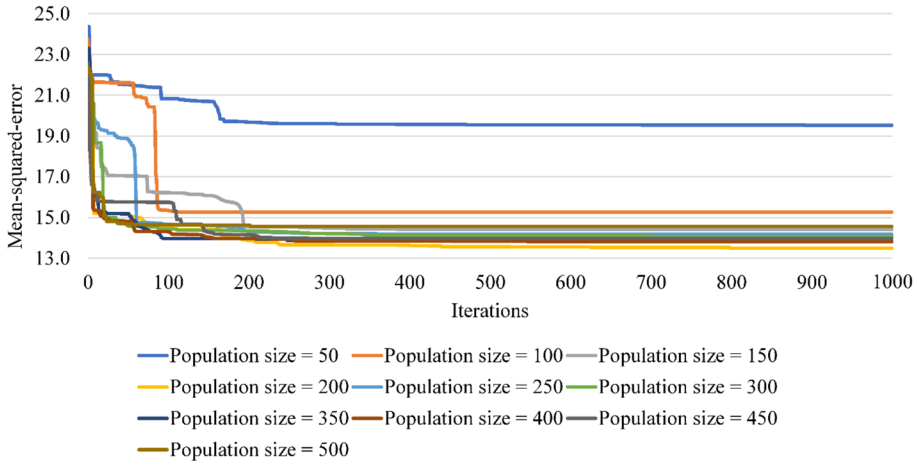

Fig. 7 Performance of the HHO algorithm in training the DMLP neural network

were applied for the RF modeling to ensure the robustness of the model. Feature scaling and tenfold cross-validation method was applied for the development of the SVM and RF model to improve the accuracy of the models. Ultimately, the results of four AI models developed are shown in Table 5. Both performances on the training and testing datasets were computed and are discussed in Table 5 to evaluate the accuracy and stability of the models.

5 Discussion

Considering the performance of the models on the training dataset, it is clear that the HHO–DMLP and DMLP models are much better than the SVM and RF models. Of those, the HHO–DMLP model is the most outstanding model with the highest performance. Remarkable, R^2 values of the SVM and RF are low (0.554 for SVM model and 0.377 for the RF model), reflecting the unsuitable of the dataset for these models. The dataset was collected from different areas/locations, and their properties are dissimilar. Therefore, with an RMSE of 3.673, R^2 of 0.777, and MAPE of 0.195%, the HHO–DMLP model can represent for the properties of the clay and friction angle of clay at different areas in this study. However, this conclusion needs to verify through the dataset in practical engineering, i.e., testing dataset. Note that the testing dataset was not used for training and developing the friction angle predictive models. In other words, they can be considered as the unseen dataset in practice.

Considering the testing dataset and the performances of the developed models, it is very interesting to note that all the predictive models are good with high performance. It is worth mentioning that the RF model provided highest accuracy on the testing dataset with an MSE of 2.786, RMSE of 1.669, R^2 of 0.961, MAPE of 0.069%, and VAF of 95.125. However, compared with the performance of the RF model on the training dataset, it is clear that the RF model was over-fitted on the testing dataset although several techniques have been applied to prevent over-fitting. Therefore, it is not reliable for predicting friction angle of clay from different areas/locations in practice. Three remaining models (i.e., HHO–DMLP, DMLP, and SVM) performed good and reliable on the testing dataset. Of those, a positive result was also found for the HHO–DMLP model on the testing dataset. With an RMSE of 3.470, R^2 of 0.796, and MAPE of 0.182% on the testing dataset, it can be concluded that the HHO–DMLP performed very well and stable in practice. Figures 8 and 9 reflect the reliability and correlation of the prediction models.

It is easy to recognize that the HHO–DMLP was fitted with the dataset over the other models (Fig. 8). Values in the range of 6 to 12 of friction angle are not fitted with the HHO–DMLP model. They should be carefully taken in predicting friction angle of clay in practical sense. On the SVM

Table 5 Performance of the friction angle predictive models

Models	Training phase					Testing phase				
	MSE	RMSE	R^2	MAPE	VAF	MSE	RMSE	R^2	MAPE	VAF
HHO–DMLP	**13.493**	**3.673**	**0.777**	**0.195**	**77.692**	**12.042**	**3.470**	**0.796**	**0.182**	**78.806**
DMLP	15.008	3.874	0.752	0.204	75.200	15.151	3.892	0.738	0.202	73.431
SVM	27.494	5.243	0.554	0.290	54.884	17.215	4.149	0.700	0.220	69.665
RF	40.001	6.325	0.377	0.304	34.329	2.786	1.669	0.961	0.069	95.125

Note: The best model for predicting friction angle is highlighted by bold type

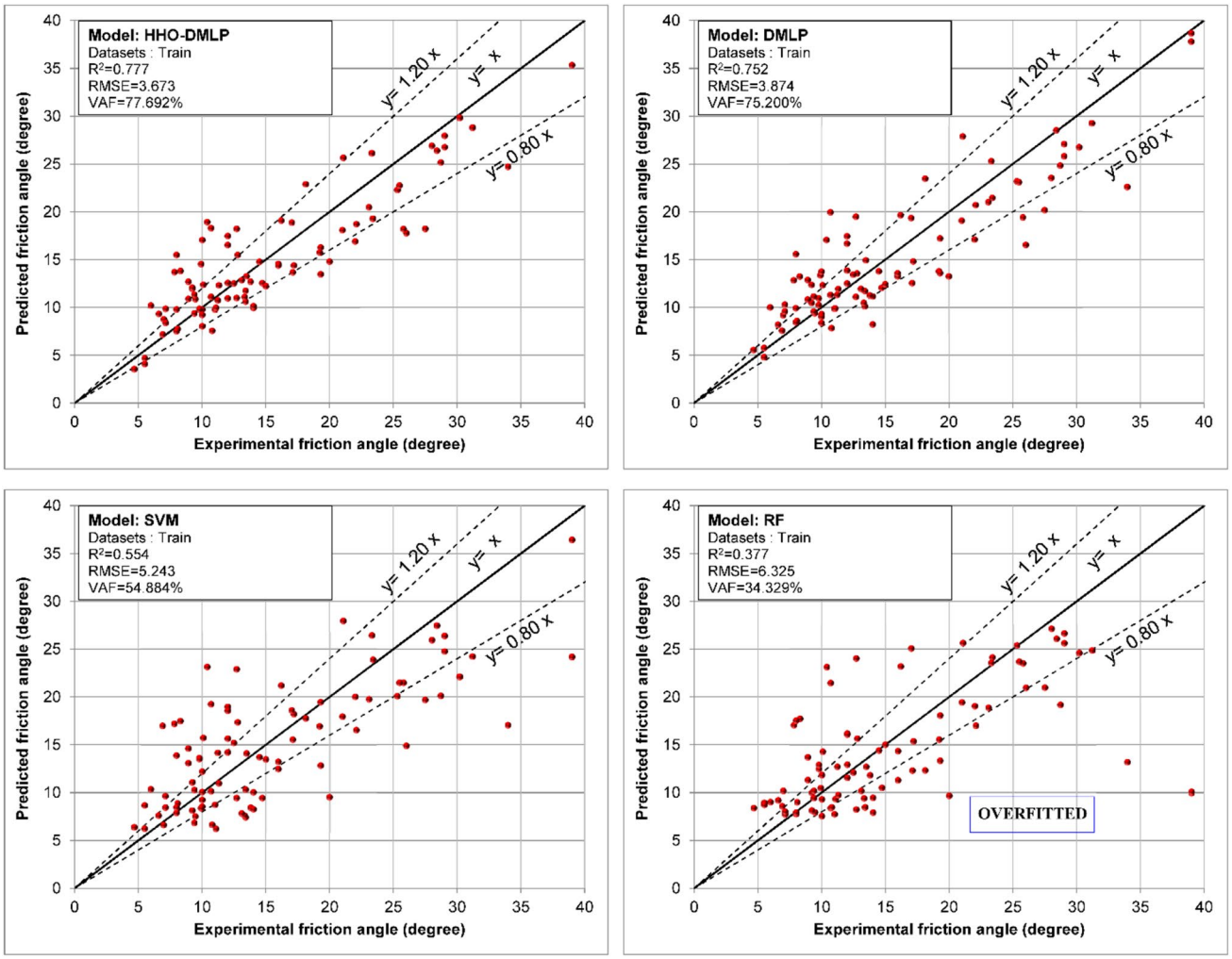

Fig. 8 Distribution of the friction angle on AI models developed (training phase)

and RF models, it is clear that the dataset is not fitted with these models and we can see that most of the observations are not converged on the regression line or 80% confidence level. Similar recommendations are achieved with the models (Fig. 9). Notably, the RF model is over-fitted in practice and it should be eliminated in predicting friction angle of clay. Based on the distribution of the dataset (Figs. 8 and 9), it can be claimed that the 80% confidence level of the proposed HHO–DMLP model can represent the friction angle of clay from different areas/locations. A comparison of the accuracy of the HHO–DMLP, DMLP (without optimization), and SVM models in predicting friction angle of clay is illustrated in Fig. 10, and further evaluation of them through the Taylor diagram is shown in Fig. 11. Note that since the RF model was over-fitted in this study, therefore, it is not compared in these figures.

From Fig. 10, it can be seen that the orange points (i.e., HHO–DMLP model) are closer to the blue points (i.e., actual values) than the other points. They indicate that the accuracy of the proposed HHO–DMLP model is higher than the remaining models in practice. Furthermore, observing the models on the Taylor diagram, we can confirm the accuracy and performance of the HHO–DMLP model as mentioned above. It is clear that the standard deviation of the actual model is high. It shows the high volatility of friction angle of clays compared to the average value, and finding a general model capable of representing the friction angle of clays at different areas/locations is not easy. The Taylor diagram showed that the HHO–DMLP model also provided high standard deviation with highest correlation. The visualization of the Taylor diagram showed that the HHO–DMLP model was closer to the actual model than the other models.

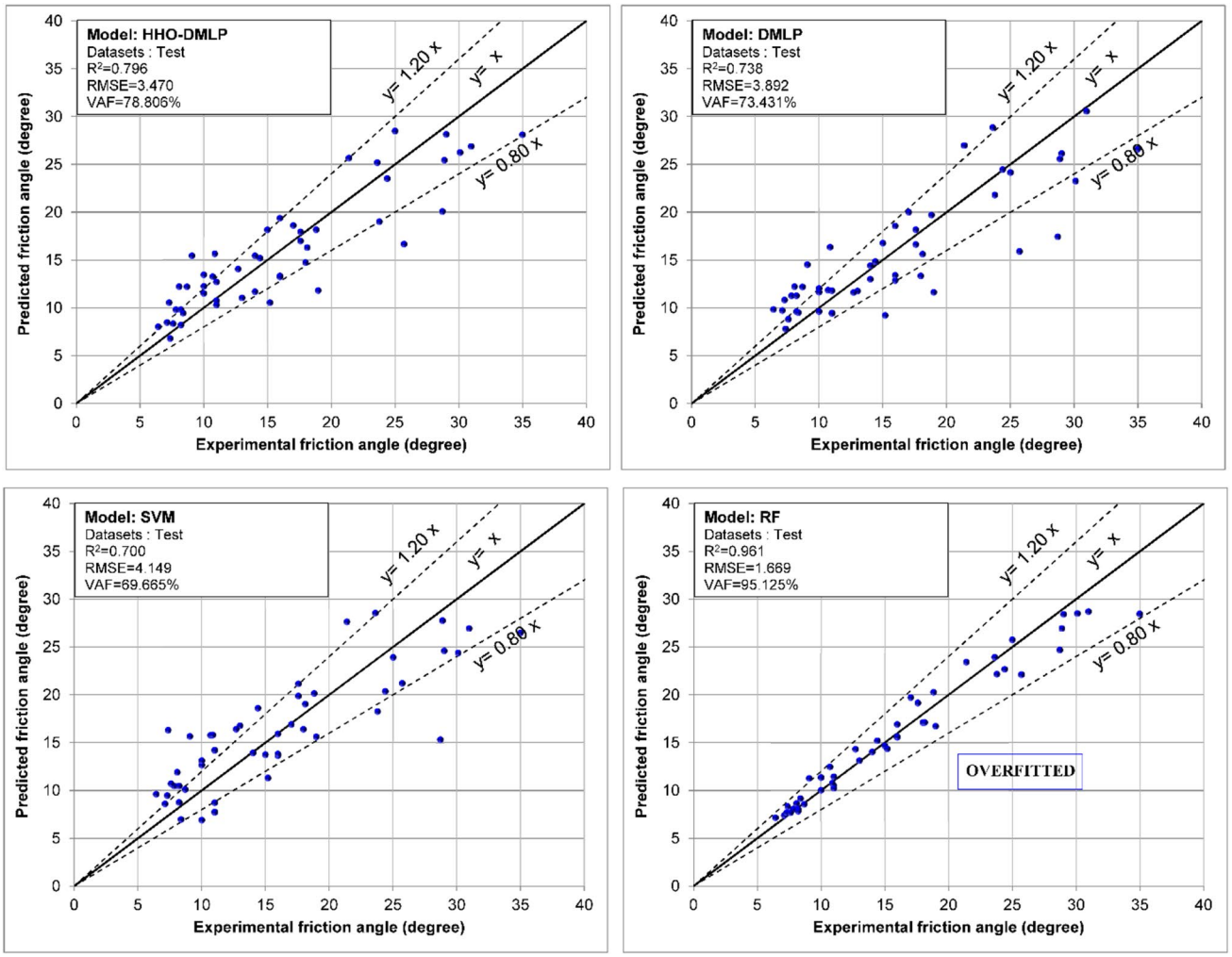

Fig. 9 Distribution of the friction angle on AI models developed (testing phase)

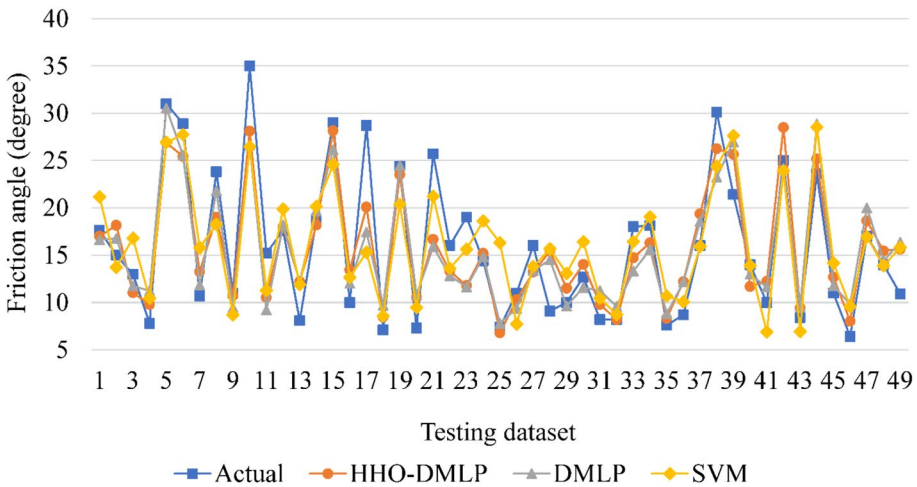

Fig. 10 Comparison of the HHO–DMLP, DMLP (without optimization), and SVM models in predicting friction angle of clay

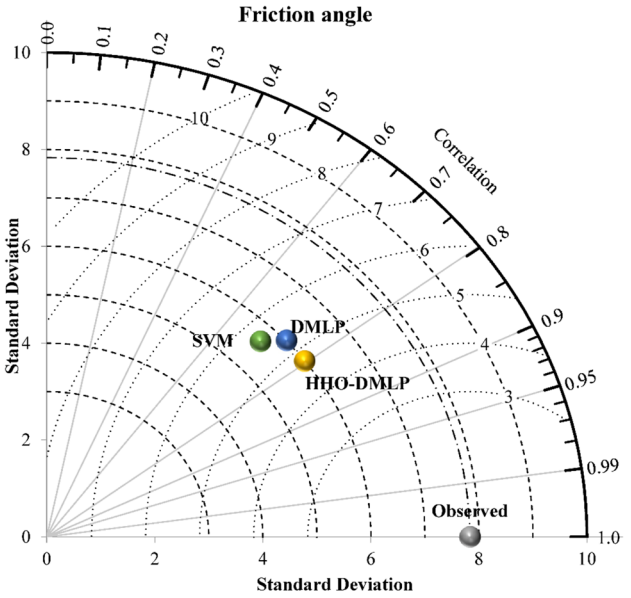

Fig. 11 Taylor diagram for proving the accuracy of the proposed HHO–DMLP model

6 Conclusion

Friction angle of clays is an essential parameter to evaluate the stability of slopes and landslide. Different areas with different clay properties have a significant influence on the stability of the slopes and landslide, especially the friction angle. Therefore, a generalized model capable of predicting friction angle of clays from different areas/locations with high reliability is ideal for assessing slope stability and landslide. This study proposed a novel generalized artificial intelligence model for estimating the friction angle of clays from different areas based on deep MLP neural network and HHO algorithm (i.e., HHO–DMLP). The robustness and consistency of the model's prediction were checked by testing with various datasets having different geological and geomorphological setups. The results showed that the proposed HHO–DMLP model can predict fiction angle of clays from different areas/locations with high reliability. It can be used in practice instead of experimental tests in a laboratory to save time and costs.

Although the obtained results are highly reliable from this study, the future work is identified with more database from other areas/locations. Future studies with more databases are useful in improving the predictive models. Such models will contribute to the current knowledge in this field and can be applied in any geographical territories.

References

1. Liu L, Li S, Li X, Jiang Y, Wei W, Wang Z, Bai Y (2019) An integrated approach for landslide susceptibility mapping by considering spatial correlation and fractal distribution of clustered landslide data. Landslides 16(4):715–728
2. Baena JAP, Scifoni S, Marsella M, De Astis G, Fernández CI (2019) Landslide susceptibility mapping on the islands of Vulcano and Lipari (Aeolian Archipelago, Italy), using a multi-classification approach on conditioning factors and a modified GIS matrix method for areas lacking in a landslide inventory. Landslides 16(5):969–982
3. Gorsevski PV, Brown MK, Panter K, Onasch CM, Simic A, Snyder J (2016) Landslide detection and susceptibility mapping using LiDAR and an artificial neural network approach: a case study in the Cuyahoga Valley National Park. Ohio Landslides 13(3):467–484
4. Salciarini D, Fanelli G, Tamagnini C (2017) A probabilistic model for rainfall—induced shallow landslide prediction at the regional scale. Landslides 14(5):1731–1746
5. Schilirò L, Montrasio L, Mugnozza GS (2016) Prediction of shallow landslide occurrence: validation of a physically-based approach through a real case study. Sci Total Environ 569:134–144
6. Chae B-G, Park H-J, Catani F, Simoni A, Berti M (2017) Landslide prediction, monitoring and early warning: a concise review of state-of-the-art. Geosci J 21(6):1033–1070
7. Montrasio L, Valentino R, Meisina C (2018) Soil saturation and stability analysis of a test site slope using the shallow landslide instability prediction (SLIP) model. Geotech Geol Eng 36(4):2331–2342
8. Dao HM, Nguyen ATT, Do TM (2020) Effect of wetting-drying cycles on surface cracking and swell-shrink behavior of expansive soil modified with ionic soil stabilizer. J Min Earth Sci 61(6):1–13
9. Pham NT, Bing P, Nguyen NV (2020) Study on the effect of some parameters of soil nails on the stability of vertical slopes. J Min Earth Sci 61(6):30–37
10. Van Pham H, Hoang PD, Ta TD (2020) Analytical methods for stress transfer efficacy in the piled embankment. J Min Earth Sci 61(6):81–87
11. Sivakumar Babu G, Srivastava A (2010) Reliability analysis of earth dams. J Geotech Geoenviron Eng 136(7):995–998
12. Tang X-S, Li D-Q, Rong G, Phoon K-K, Zhou C-B (2013) Impact of copula selection on geotechnical reliability under incomplete probability information. Comput Geotech 49:264–278
13. Renani HR, Martin CD (2018) Cohesion degradation and friction mobilization in brittle failure of rocks. Int J Rock Mech Min Sci 106:1–13
14. Stockton E, Leshchinsky BA, Olsen MJ, Evans TM (2019) Influence of both anisotropic friction and cohesion on the formation of tension cracks and stability of slopes. Eng Geol 249:31–44
15. Kulhawy FH, Mayne PW (1990) Manual on estimating soil properties for foundation design. In: Electric Power Research Inst., Palo Alto, CA (USA). Cornell Univ., Ithaca
16. Ameratunga J, Sivakugan N, Das BM (2016) Correlations of soil and rock properties in geotechnical engineering. Springer, Berlin
17. Ahmadipur A, Qiu T, Sheikh B (2019) Investigation of basal friction effects on impact force from a granular sliding mass to a rigid obstruction. Landslides 16(6):1089–1105
18. Abdelmalak M, Bulois C, Mourgues R, Galland O, Legland J-B, Gruber C (2016) Description of new dry granular materials of variable cohesion and friction coefficient: Implications for laboratory modeling of the brittle crust. Tectonophysics 684:39–51
19. Zhang J, Ju Y, Zhou C (2013) Experimental research on cohesion and internal friction angle of the double-base propellant. Propell Explos Pyrotech 38(3):351–357
20. Merchán V, Vaunat J, Romero E, Meca T (2008) Experimental study of the influence of suction on the residual friction angle of clays. CRC Press,

21. Arvanitidis C, Steiakakis E, Agioutantis Z (2019) Peak Friction Angle of Soils as a Function of Grain Size. Geotech Geol Eng 37(3):1155–1167
22. Jiang H, Xie Y (2011) A note on the Mohr-Coulomb and Drucker-Prager strength criteria. Mech Res Commun 38(4):309–314
23. Yamada M, Mangeney A, Matsushi Y, Matsuzawa T (2018) Estimation of dynamic friction and movement history of large landslides. Landslides 15(10):1963–1974
24. Nguyen TA, Van Pham V, Bui NX, Le HTT, Le HT, Tran BD, Le HMT (2020) Modelisation of fractured rock mass for open pit mining in Vietnam. J Min Earth Sci 61(5):80–96
25. Hazelton P, Murphy B (2016) Interpreting soil test results: What do all the numbers mean? CSIRO publishing, Clayton
26. Bell FG (2013) Engineering properties of soils and rocks. Elsevier, Amsterdam
27. Bui X-N, Nguyen H, Choi Y, Nguyen-Thoi T, Zhou J, Dou J (2020) Prediction of slope failure in open-pit mines using a novel hybrid artificial intelligence model based on decision tree and evolution algorithm. Sci Rep 10(1)
28. Zhou J, Li E, Yang S, Wang M, Shi X, Yao S, Mitri HS (2019) Slope stability prediction for circular mode failure using gradient boosting machine approach based on an updated database of case histories. Saf Sci 118:505–518
29. Garven E, Vanapalli S (2006) Evaluation of empirical procedures for predicting the shear strength of unsaturated soils. Unsaturated Soils 2006:2570–2592
30. Kaya A, Kwong JK (2007) Evaluation of common practice empirical procedures for residual friction angle of soils: Hawaiian amorphous material rich colluvial soil case study. Eng Geol 92(1–2):49–58
31. Borykov T, Mège D, Mangeney A, Richard P, Gurgurewicz J, Lucas A (2019) Empirical investigation of friction weakening of terrestrial and Martian landslides using discrete element models. Landslides 16(6):1121–1140
32. Nguyen H, Bui X-N (2020) Soft computing models for predicting blast-induced air over-pressure: A novel artificial intelligence approach. Appl Soft Comput 92:106292. https://doi.org/10.1016/j.asoc.2020.106292
33. Nguyen H, Bui X-N, Tran Q-H, Mai N-L (2019) A new soft computing model for estimating and controlling blast-produced ground vibration based on hierarchical K-means clustering and cubist algorithms. Applied Soft Computing 77:376–386. https://doi.org/10.1016/j.asoc.2019.01.042
34. Nguyen H, Bui X-N, Bui H-B, Cuong DT (2019) Developing an XGBoost model to predict blast-induced peak particle velocity in an open-pit mine: a case study. Acta Geophys 67(2):477–490. https://doi.org/10.1007/s11600-019-00268-4
35. Bui X-N, Lee CW, Nguyen H, Bui H-B, Long NQ, Le Q-T, Nguyen V-D, Nguyen N-B, Moayedi H (2019) Estimating PM10 concentration from drilling operations in open-pit mines using an assembly of SVR and PSO. Appl Sci 9(14):2806
36. Bui X-N, Nguyen H, Le H-A, Bui H-B, Do N-H (2019) Prediction of blast-induced air over-pressure in open-pit mine: assessment of different artificial intelligence techniques. Nat Resour Res 29(2):571–591. https://doi.org/10.1007/s11053-019-09461-0
37. Guo H, Nguyen H, Vu D-A, Bui X-N (2019) Forecasting mining capital cost for open-pit mining projects based on artificial neural network approach. Resour Policy. https://doi.org/10.1016/j.resourpol.2019.101474
38. Nguyen H, Drebenstedt C, Bui X-N, Bui DT (2019) Prediction of blast-induced ground vibration in an open-pit mine by a novel hybrid model based on clustering and artificial neural network. Nat Resour Res 29(2):691–709. https://doi.org/10.1007/s11053-019-09470-z
39. Zhang X, Nguyen H, Bui X-N, Tran Q-H, Nguyen D-A, Bui DT, Moayedi H (2019) Novel soft computing model for predicting blast-induced ground vibration in open-pit mines based on particle swarm optimization and XGBoost. Nat Resour Res 29(2):711–721. https://doi.org/10.1007/s11053-019-09492-7
40. Shang Y, Nguyen H, Bui X-N, Tran Q-H, Moayedi H (2019) A novel artificial intelligence approach to predict blast-induced ground vibration in open-pit mines based on the firefly algorithm and artificial neural network. Nat Resour Res 29(2):723–737. https://doi.org/10.1007/s11053-019-09503-7
41. Rashid QA, Abuel-Naga H, Leong E-C, Lu Y, Al Abadi H (2018) Experimental-artificial intelligence approach for characterizing electrical resistivity of partially saturated clay liners. Appl Clay Sci 156:1–10
42. Das SK, Basudhar PK (2008) Prediction of residual friction angle of clays using artificial neural network. Eng Geol 100(3–4):142–145
43. Das S, Samui P, Khan S, Sivakugan N (2011) Machine learning techniques applied to prediction of residual strength of clay. Open Geosci 3(4):449–461
44. Khan S, Suman S, Pavani M, Das S (2016) Prediction of the residual strength of clay using functional networks. Geosci Front 7(1):67–74
45. Casagrande D, Buzzi O, Giacomini A, Lambert C, Fenton G (2018) A new stochastic approach to predict peak and residual shear strength of natural rock discontinuities. Rock Mech Rock Eng 51(1):69–99
46. Pham BT, Hoang T-A, Nguyen D-M, Bui DT (2018) Prediction of shear strength of soft soil using machine learning methods. CATENA 166:181–191
47. Matos Y, Neto SD, Barreto G (2019) Predicting the shear strength of unfilled rock joints with the first-order Takagi-Sugeno fuzzy approach. Soils Rocks, p 21
48. Nguyen H, Bui X-N (2019) Predicting blast-induced air overpressure: a robust artificial intelligence system based on artificial neural networks and random forest. Nat Resour Res 28(3):893–907. https://doi.org/10.1007/s11053-018-9424-1
49. Nguyen H, Bui X-N, Tran Q-H, Moayedi H (2019) Predicting blast-induced peak particle velocity using BGAMs, ANN and SVM: a case study at the Nui Beo open-pit coal mine in Vietnam. Environ Earth Sci 78(15):479. https://doi.org/10.1007/s12665-019-8491-x
50. Nguyen H (2019) Support vector regression approach with different kernel functions for predicting blast-induced ground vibration: a case study in an open-pit coal mine of Vietnam. SN Appl Sci 1(4):283
51. Nguyen H, Bui X-N, Moayedi H (2019) A comparison of advanced computational models and experimental techniques in predicting blast-induced ground vibration in open-pit coal mine. Acta Geophys 67(4):1025–1037. https://doi.org/10.1007/s11600-019-00304-3
52. Zhou J, Qiu Y, Armaghani DJ, Zhang W, Li C, Zhu S, Tarinejad R (2021) Predicting TBM penetration rate in hard rock condition: A comparative study among six XGB-based metaheuristic techniques. Geosci Front 12(3):101091
53. Zhou J, Qiu Y, Zhu S, Armaghani DJ, Li C, Nguyen H, Yagiz S (2021) Optimization of support vector machine through the use of metaheuristic algorithms in forecasting TBM advance rate. Eng Appl Artif Intell 97:104015
54. Nguyen H, Bui X-N, Bui H-B, Mai N-L (2018) A comparative study of artificial neural networks in predicting blast-induced air-blast overpressure at Deo Nai open-pit coal mine. VietNeural Comput Appl 32(8):3939–3955. https://doi.org/10.1007/s00521-018-3717-5
55. Liu W, Moayedi H, Nguyen H, Lyu Z, Bui DT (2019) Proposing two new metaheuristic algorithms of ALO-MLP and SHO-MLP in predicting bearing capacity of circular footing located on horizontal multilayer soil. Eng Comput, 1–11

56. Moayedi H, Nguyen H, Foong LK (2019) Nonlinear evolutionary swarm intelligence of grasshopper optimization algorithm and gray wolf optimization for weight adjustment of neural network. Eng Comput, pp 1–11
57. Hecht-Nielsen R (1992) Theory of the backpropagation neural network. In: Neural networks for perception. Elsevier, pp 65–93
58. Kwok T-Y, Yeung D-Y (1997) Constructive algorithms for structure learning in feedforward neural networks for regression problems. IEEE Trans Neural Netw 8(3):630–645
59. Chan KY, Dillon TS, Singh J, Chang E (2011) Neural-network-based models for short-term traffic flow forecasting using a hybrid exponential smoothing and Levenberg–Marquardt algorithm. IEEE Trans Intell Transp Syst 13(2):644–654
60. Liu W, Wang Z, Liu X, Zeng N, Liu Y, Alsaadi FE (2017) A survey of deep neural network architectures and their applications. Neurocomputing 234:11–26
61. Schmidhuber J (2015) Deep learning in neural networks: An overview. Neural Netw 61:85–117
62. Nielsen MA (2015) Neural networks and deep learning, vol 2018. Determination Press, San Francisco
63. Goodfellow I, Bengio Y, Courville A (2016) Deep learning. MIT press, Cambrdige
64. Zhang H, Nguyen H, Bui X-N, Nguyen-Thoi T, Bui T-T, Nguyen N, Vu D-A, Mahesh V, Moayedi H (2020) Developing a novel artificial intelligence model to estimate the capital cost of mining projects using deep neural network-based ant colony optimization algorithm. Resour Policy 66:101604
65. Nguyen H, Bui X-N, Nguyen-Thoi T, Ragam P, Moayedi H (2019) Toward a state-of-the-art of fly-rock prediction technology in open-pit mines using EANNs model. Appl Sci 9(21):4554
66. Armenteros JJA, Tsirigos KD, Sønderby CK, Petersen TN, Winther O, Brunak S, von Heijne G, Nielsen H (2019) SignalP 5.0 improves signal peptide predictions using deep neural networks. Nat Biotechnol 37(4):420–423
67. Bouwmans T, Javed S, Sultana M, Jung SK (2019) Deep neural network concepts for background subtraction: A systematic review and comparative evaluation. Neural Networks
68. Nie S, Xue L, Jia G, Ma Y, Chen J, Huo J (2019) Identification of surrounding rock in TBM excavation with deep neural network. In: 2019 2nd International Conference on Artificial Intelligence and Big Data (ICAIBD), 2019. IEEE, pp 251–255
69. Guo H, Zhou J, Koopialipoor M, Armaghani DJ, Tahir M (2019) Deep neural network and whale optimization algorithm to assess flyrock induced by blasting. Eng Comput, pp 1–14
70. Luo L, Bai Z, Zhu W, Sun J (2018) Improved functional link artificial neural network filters for nonlinear active noise control. Appl Acoust 135:111–123
71. Eckle K, Schmidt-Hieber J (2019) A comparison of deep networks with ReLU activation function and linear spline-type methods. Neural Netw 110:232–242
72. Ide H, Kurita T Improvement of learning for CNN with ReLU activation by sparse regularization. In: 2017 International Joint Conference on Neural Networks (IJCNN), 2017. IEEE, pp 2684–2691
73. Lin G, Shen W (2018) Research on convolutional neural network based on improved Relu piecewise activation function. Proc Comput Sci 131:977–984
74. Yarotsky D (2017) Error bounds for approximations with deep ReLU networks. Neural Netw 94:103–114
75. Petersen P, Voigtlaender F (2018) Optimal approximation of piecewise smooth functions using deep ReLU neural networks. Neural Netw 108:296–330
76. Zou D, Cao Y, Zhou D, Gu Q (2020) Gradient descent optimizes over-parameterized deep ReLU networks. Mach Learn 109(3):467–492
77. Heidari AA, Mirjalili S, Faris H, Aljarah I, Mafarja M, Chen H (2019) Harris hawks optimization: Algorithm and applications. Future GenerComput Syst 97:849–872
78. Moayedi H, Nguyen H, Rashid ASA (2019) Comparison of dragonfly algorithm and Harris hawks optimization evolutionary data mining techniques for the assessment of bearing capacity of footings over two-layer foundation soils. Eng Comput, pp 1–11
79. Yıldız BS, Yıldız AR (2019) The Harris hawks optimization algorithm, salp swarm algorithm, grasshopper optimization algorithm and dragonfly algorithm for structural design optimization of vehicle components. Mater Testing 61(8):744–748
80. Golilarz NA, Gao H, Demirel H (2019) Satellite image de-noising with Harris hawks meta heuristic optimization algorithm and improved adaptive generalized gaussian distribution threshold function. IEEE Access 7:57459–57468
81. Moayedi H, Osouli A, Nguyen H, Rashid ASA (2019) A novel Harris hawks' optimization and k-fold cross-validation predicting slope stability. Eng Comput, pp 1–11
82. Houssein EH, Saad MR, Hussain K, Zhu W, Shaban H, Hassaballah M (2020) Optimal sink node placement in large scale wireless sensor networks based on Harris' hawk optimization algorithm. IEEE Access 8:19381–19397
83. Wesley L (2003) Residual strength of clays and correlations using Atterberg limits. Geotechnique 53(7):669–672
84. Tiwari B, Marui H (2005) A new method for the correlation of residual shear strength of the soil with mineralogical composition. J Geotech Geoenviron Eng 131(9):1139–1150
85. Skempton AW (1985) Residual strength of clays in landslides, folded strata and the laboratory. Geotechnique 35(1):3–18
86. Meisina C (2010) Relationship between the residual shear strength and the methylene blue value in weathered clay soils. Geol Soc Lond Eng Geol Sp Publ 23(1):213–233

Authors and Affiliations

Hong Zhang[1] · Hoang Nguyen[2] · Xuan-Nam Bui[2,3] · Biswajeet Pradhan[4,5] · Panagiotis G. Asteris[6] · Romulus Costache[7,8] · Jagannath Aryal[9]

[1] Department of Economics and Management, Changsha University, Changsha, China

[2] Department of Surface Mining, Mining Faculty, Hanoi University of Mining and Geology, 18 Vien st., Duc Thang ward, Bac Tu Liem dist., Hanoi, Vietnam

[3] Center for Mining, Electro-Mechanical Research, Hanoi University of Mining and Geology, 18 Vien st., Duc Thang ward, Bac Tu Liem dist., Hanoi, Vietnam

[4] The Centre for Advanced Modelling and Geospatial Information Systems (CAMGIS), School of Information, Systems and Modelling, University of Technology, Sydney, NSW 2007, Australia

[5] Department of Energy and Mineral Resources Engineering, Sejong University, Choongmu-gwan, 209 Neungdong-ro, Gwangjingu, Seoul 05006, South Korea

[6] Computational Mechanics Laboratory, School of Pedagogical and Technological Education, Heraklion, 14121 Athens, Greece

[7] Research Institute of the University of Bucharest, 90-92 Sos. Panduri, 5th District, Bucharest, Romania

[8] National Institute of Hydrology and Water Management, București-Ploiești Road, 97E, 1st District, 013686 Bucharest, Romania

[9] Melbourne School of Engineering, University of Melbourne, Victoria, Australia